Stem Cell Research (2011) 6, 129–142

available at www.sciencedirect.com

www.elsevier.com/locate/scr

REGULAR ARTICLE

A high-throughput multiplexed screening assay for optimizing serum-free differentiation protocols of human embryonic stem cells

Joel T. Outten[a,b], Xin Cheng[c], Paul Gadue[c], Deborah L. French[c], Scott L. Diamond[a,b,d,*]

[a] Institute for Medicine and Engineering, University of Pennsylvania, Philadelphia, PA 19104, USA
[b] Departments of Bioengineering, University of Pennsylvania, Philadelphia, PA 19104, USA
[c] Department of Pathology, Center for Cellular and Molecular Therapeutics, Children's Hospital of Philadelphia, Philadelphia, PA, USA
[d] Chemical and Biomolecular Engineering, University of Pennsylvania, Philadelphia, PA 19104, USA

Received 28 May 2010; received in revised form 21 October 2010; accepted 8 November 2010
Available online 16 November 2010

Abstract Serum-free differentiation protocols of human embryonic stem cells (hESCs) offer the ability to maximize reproducibility and to develop clinically applicable therapies. We developed a high-throughput, 96-well plate, four-color flow cytometry-based assay to optimize differentiation media cocktails and to screen a variety of conditions. We were able to differentiate hESCs to all three primary germ layers, screen for the effect of a range of activin A, BMP4, and VEGF concentrations on endoderm and mesoderm differentiation, and perform RNA-interference (RNAi)-mediated knockdown of a reporter gene during differentiation. Cells were seeded in suspension culture and embryoid bodies were induced to differentiate to the three primary germ layers for 6 days. Endoderm ($CXCR4^+KDR^-$), mesoderm ($KDR^+SSEA\text{-}3^-$), and ectoderm ($SSEA\text{-}3^+NCAM^+$) differentiation yields for H9 cells were 80±11, 78±7, and 41±9%, respectively. Germ layer identities were confirmed by quantitative PCR. Activin A, BMP4, and bFGF drove differentiation, with increasing concentrations of activin A inducing higher endoderm yields and increasing BMP4 inducing higher mesoderm yields. VEGF drove lateral mesoderm differentiation. RNAi-mediated knockdown of constitutively expressed red fluorescent protein did not affect endoderm differentiation. This assay facilitates the development of serum-free protocols for hESC differentiation to target lineages and creates a platform for screening small molecules or RNAi during ESC differentiation.

Introduction

Human embryonic stem cells (hESCs) offer the potential to regenerate any cell in the human body. Initially, many studies utilized serum-containing media to develop differentiation protocols for target cell types (D'Amour et al., 2006; Kyba et al., 2002; Reubinoff et al., 2000; Zambidis et al., 2005). Serum, however, contains unknown and variable concentrations of growth factors and proteins. More recently, serum-free differentiation (SFD) protocols have emerged in order to

* Corresponding author. Institute for Medicine and Engineering, University of Pennsylvania, 1024 Vagelos Laboratory, 3340 Smith Walk, University of Pennsylvania, Philadelphia, PA 19104, USA. Fax: +1 215 573 6815.
E-mail address: sld@seas.upenn.edu (S.L. Diamond).

1873-5061/$ – see front matter © 2010 Elsevier B.V. All rights reserved.
doi:10.1016/j.scr.2010.11.001

maximize reproducibility and to gain a more thorough understanding of biological pathways activated during differentiation to specified lineages (Kennedy et al., 2007; Matsumoto et al., 2009; Nakanishi et al., 2009; Park et al., 2004). Numerous combinations of cytokines, growth factors, and siRNA molecules are being evaluated in order to understand signaling pathways utilized during differentiation and to optimize differentiation protocols to target cell types. By precisely activating or inhibiting the TGFβ family, FGF, Wnt, and other pathways at specific times, the developing embryo directs differentiation to all somatic cells of the body (Gadue et al., 2005). *In vitro* hESC differentiation systems attempt to recapitulate these developmental pathways by utilizing controlled concentrations of cytokines and inhibitors. As differentiation proceeds down specific lineages, the possible number of cytokine combinations dramatically increases. A high-throughput screening method that streamlines the analysis of various growth factor combinations and their effect on differentiation would be extremely beneficial.

Only a few groups have developed small-scale ESC differentiation systems in order to probe biological pathways and optimize differentiation media cocktails. Ng et al. (Ng et al., 2005, 2008) have developed a 96-well spin embryoid body (EB) technique in which hESCs are spun down to form a single EB of a defined size within each well. This technique has been utilized to optimize differentiation to various stages in the hematopoietic lineage (Pick et al., 2007; Davis et al., 2008). Koike et al. have developed a 96-well murine ESC (mESC) differentiation system and explored the effects of EB seeding density on differentiation to cardiomyocytes (Koike et al., 2005, 2007). Due to the small seeding density utilized by both methods to generate single EBs and the tendency for cell counts to drop over the first 5 days of differentiation (Pick et al., 2007), it is unclear if enough cells would be available for 96-well flow cytometry analyses without pooling wells. Several studies have utilized an adherent 384-well plate format to screen for small molecule inhibitors or enhancers of ESC differentiation (Borowiak et al., 2009; Desbordes et al., 2008). Although these confocal microscopy-based assays have been utilized to screen several thousand small molecules, they are not conducive to multicolor flow cytometry or live cell sorting.

RNA interference (RNAi)-mediated gene knockdown has also become a common technique to explore gene involvement in active pathways. siRNA knockdown of reporter genes does not affect pluripotency in hESCs grown on mouse embryonic fibroblasts (MEFs) (Vallier et al., 2004). Knockdown of *OCT4* and *NANOG* has been shown to induce differentiation and loss of pluripotency in hESCs (Hay et al., 2004; Zaehres et al., 2005; Rodriguez et al., 2007). RNAi has been utilized to elucidate signaling pathways that mediate ESC differentiation to multiple lineages (Izumi et al., 2007). Despite the potential that RNAi offers for understanding biology and modifying pathway activation, there are little data available regarding any potential off-target effects this technique may have on targeted hESC differentiation.

We have developed a small-scale, flow cytometry-based, high-throughput hESC EB differentiation assay. In this study, we differentiate hESCs to the three primary germ layers and demonstrate biomarker profiles unique to each cell type. We obtained high cell yields for each layer with remarkably low well-to-well variability. We also demonstrate the ability to perform small interfering RNA (siRNA)-mediated gene knockdown at this scale without disrupting induced differentiation. These results demonstrate the utility and efficacy of this system for efficiently optimizing SFD conditions and performing siRNA knockdown on numerous targets.

Results

EB differentiation in a 96-well format

We optimized a 96-well plate, four-color flow cytometry assay for analyzing surface markers during hESC EB differentiation into target lineages. A stepwise EB differentiation protocol was modified to differentiate the cells for 6 days (Fig. 1A) (Yang et al., 2008). A four-color biomarker-based flow cytometry assay to detect cells representative of all three primary germ layers and undifferentiated hESCs in a single sample was developed (Fig. 1B). Combinations of the surface markers CXCR4, KDR, NCAM, and SSEA-3 were assessed to distinguish each cell type. CXCR4 is a reliable marker for definitive endoderm (Yasunaga et al., 2005), but is also expressed in migrating mesoderm (McGrath et al., 1999). KDR has frequently been utilized to characterize early mesoderm prior to diverging to a KDR^+ lateral lineage or a $PDGFR\alpha^+$ paraxial lineage (Nostro et al., 2008; Sakurai et al., 2006) and is also expressed at low levels by hESCs (Yang et al., 2008). SSEA-3 is a marker of pluripotency expressed by hESCs. On differentiation, SSEA-3 expression is lost (Enver et al., 2005; Kannagi et al., 1983), although expression is maintained at the early neuroectoderm, neural stem cell stage (Pruszak et al., 2007). NCAM (or CD56) is a neural marker whose expression is induced during this early ectoderm stage (Pruszak et al., 2007) and is a general marker for ectoderm differentiation (Park et al., 2008). However, NCAM expression is not unique to ectoderm but is expressed by some endoderm and mesoderm cells as well (Lackie et al., 1994; Moller et al., 1992). Therefore, we utilized $SSEA\text{-}3^+NCAM^-$ expression to characterize hESCs, $CXCR4^+KDR^-$ expression for endoderm, $SSEA\text{-}3^+NCAM^+$ expression for ectoderm, and $KDR^+SSEA\text{-}3^-$ expression for mesoderm.

In order to examine interwell variability and percentage differentiation, one 96-well plate was partitioned into three induction media zones: endoderm, mesoderm, and ectoderm. We utilized high activin A with bFGF to induce endoderm (D'Amour et al., 2006), high BMP4 with bFGF to induce mesoderm (Yang et al., 2008), and simultaneous activin inhibition (SB431542) and BMP4 inhibition (BMP receptor 1A; BMPR1A) with bFGF to induce ectoderm (Chambers et al., 2009; Vallier et al., 2009) (Fig. 1B). The EBs appeared robust and morphologically similar to those grown in bacterial grade dishes and 6-well plates. A Ninety-six well flow cytometry was performed and the different populations of cells were defined from expression of the four biomarkers (Figs. 2A and B, Fig. S1). HES2 endoderm ($CXCR4^+KDR^-$), mesoderm ($KDR^+SSEA\text{-}3^-$), and ectoderm ($SSEA\text{-}3^+NCAM^+$) differentiation yields were 74 ± 9, 74 ± 17, and 57 ± 8%, respectively (Fig. 3E). H9 cells demonstrated similar yields of 80 ± 11, 78 ± 7, and 41 ± 9% for endoderm, mesoderm, and ectoderm, respectively (Fig. 3F). Interwell variability was remarkably low between identical induction conditions (Figs. 3A–D), with standard deviations consistently less than 4%. Activin-/BMP-inhibited media

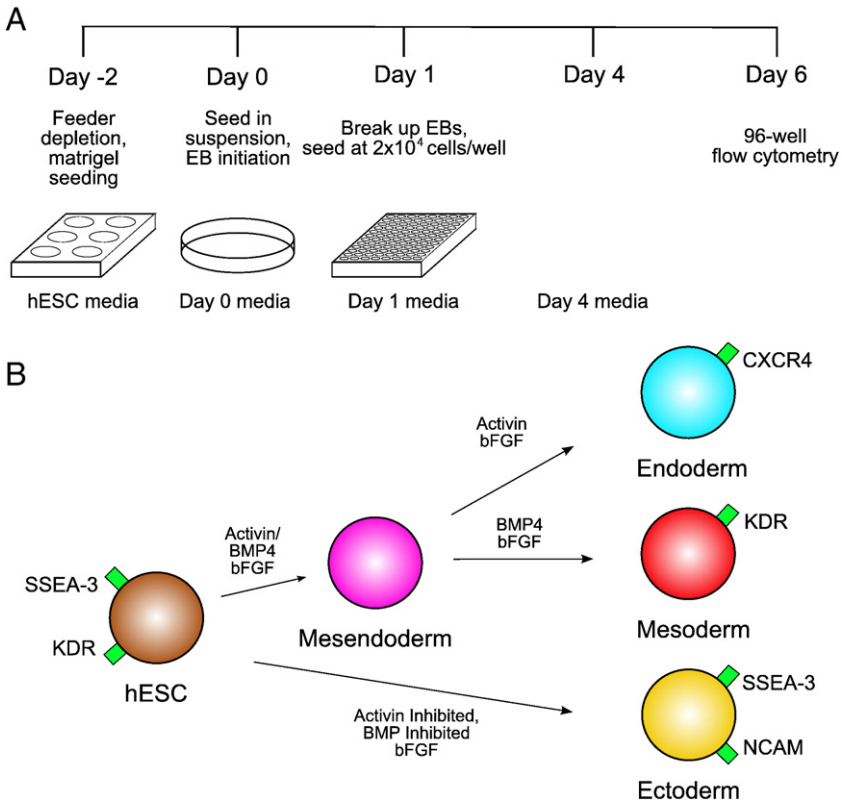

Figure 1 Experiment schematic and differentiation model. (A) The 6-day stepwise hESC EB differentiation schematic. Differentiation protocols were established in which cells were fed at Days 0, 1, and 4. Cells were seeded into 96-well plates at Day 1 and analyzed by 96-well flow cytometry at Day 6. (B) Differentiation and biomarker expression model. A four-biomarker combination was designed in which hESCs and cells representing the three primary germ layers could be analyzed in a single sample. Abbreviations: hESCs, human embryonic stem cells; EB, embryoid body; SSEA-3, stage-specific embryonic antigen-3; CXCR, CXC chemokine receptor; KDR, kinase insert domain receptor; NCAM, neural cell adhesion molecule; BMP, bone morphogenetic protein; bFGF, basic fibroblast growth factor.

retained expression characteristics of undifferentiated hESCs ($28 \pm 17\%$ SSEA-3$^+$NCAM$^-$), although NANOG and OCT4 transcript expression indicated that this is likely due to retained expression of SSEA-3 in non-NCAM expressing ectoderm (Fig. 2C).

Cells displayed some toxicity after being seeded at Day 0 and then demonstrated proliferation after 2 days of differentiation (Fig. S2). Both endoderm and mesoderm conditions yielded 4- to 6-day cell counts similar to the initial seeding density of 2×10^4 cells/well, indicating a potential population plateau for these media. Ectoderm cell yields (Day 6 cell counts compared to Day 0 seeding densities) were greater than 300% at Day 6, possibly attributable to the addition of 20 ng/ml bFGF at Day 4. In order to evaluate the effect of seeding density on differentiation efficiency, we evaluated Day 6 marker expression levels for seeding densities of 8×10^3 to 6×10^4 cells/well (Fig. S3). The assay proved to be highly robust for differences in cell densities. Undifferentiated populations increased with increasing densities, as expected due to nutrient and cytokine depletion. Mesoderm and ectoderm differentiation efficiency showed a gradual decreasing trend with increasing seeding density, whereas endoderm efficiency was essentially constant.

The differentiated populations of cells representative of each primary germ layer, as well as undifferentiated hESCs, display a unique biomarker profile (Figs. 3E and F). Each cell type was distinguished by increased expression of a combination of biomarkers. These findings suggest that this four-biomarker assay can be utilized to distinguish four unique cell types after 6 days of differentiation. Furthermore, the three differentiated cell types have a biomarker profile characteristic of endodermal, mesodermal, or early ectodermal cells.

Gene expression verification of induced germ layers

In order to verify that the surface marker profiles obtained using flow cytometry corresponded to the anticipated lineages, real-time quantitative PCR (qPCR) was performed on RNA harvested from Day 0 hESCs and from cells after 6 days of differentiation under the various differentiation conditions. The pluripotency genes *NANOG* and *OCT4* were expressed in undifferentiated cells and as expected were downregulated under the three conditions inducing cellular differentiation (Fig. 2C). The anterior primitive streak gene *FOXA2* was drastically upregulated under the high activin endoderm induction conditions, as were the anterior definitive endoderm genes *SOX17* and *CER1* (Fig. 2D). Fig. 2E displays characteristic gene expression profiles representative of cells within the posterior primitive streak and differentiating toward mesoderm. These genes were

upregulated under conditions using high BMP4, and are representative of early stage as well as paraxial (*PDGFRα*) and lateral progenitor mesoderm (*GATA2*) (Fig. 2E). Dual BMP4 and activin A inhibition increased both *PAX6* and *SOX1* transcript expression (Fig. 2F). The neuronal marker *NESTIN* was not upregulated under the ectoderm induction conditions, indicating that these cells have not yet begun to undergo neuralization (Lendahl et al., 1990). These gene expression data support the flow cytometry profiles showing that the three defined induction conditions differentiate the cells into lineages representative of endodermal, mesodermal, and early ectodermal germ layers.

Growth factor screening assay

We next sought to apply the 96-well flow cytometry assay to efficiently screen specific growth factors across a range of concentrations. The concentrations of three growth factors, activin A (0–100 ng/ml), BMP4 (0–40 ng/ml), and VEGF (± 10 ng/ml), were assessed for differentiation to endoderm and mesoderm over the course of 6 days. The expression of PDGFRα was assessed for an additional mesodermal marker and to indicate early progression toward the paraxial germ layer (Sakurai et al., 2006). As discussed previously, $SSEA3^+$, $CXCR4^+KDR^-$, and $KDR^+SSEA\text{-}3^-$ expression was used to indicate undifferentiated cells and commitment of cells to endoderm and mesoderm, respectively. As expected, expression of the pluripotency marker, SSEA-3, steadily decreased under conditions with increasing concentrations of activin and BMP4 (Fig. 4A). $CXCR4^+KDR^-$ expression was nonexistent in the absence of activin A, whereas a low concentration of activin A (10 ng/ml) was sufficient to induce high (>60% of cells) CXCR4 expression (Fig. 4B). Increasing activin A from 10 to 100 ng/ml increased $CXCR4^+KDR^-$ expression for high BMP4 conditions, but otherwise did not have a notable effect on $CXCR4^+KDR^-$ expression. For a constant activin A concentration, increasing BMP4 consistently reduced CXCR4 expression. $PDGFR\alpha^+$ and KDR^+ populations were greatest in the absence of activin A (Figs. 4C and D). Increasing the activin A concentration immediately abrogated PDGFRα expression. Activin A and BMP4 displayed a competitive relationship on $KDR^+SSEA\text{-}3^-$ expression. Increasing BMP4 concentration increased KDR expression, whereas activin A consistently inhibited this expression. Under most conditions, the additional supplementation of 10 ng/ml VEGF had no notable effect on the expression of this set of cell surface markers (Figs. 4A–D).

These data suggest this 96-well flow cytometry assay can be utilized to screen for the effect of a spectrum of growth factor concentrations on hESC differentiation under serum-free conditions. Furthermore, increased concentrations of both activin A and BMP4 reduce pluripotency. Increasing activin A concentration increases $CXCR4^+KDR^-$ endoderm populations and reduces both $KDR^+SSEA\text{-}3^-$ and $PDGFR\alpha^+$ mesoderm populations. Conversely, increasing BMP4 concentration increases $KDR^+SSEA\text{-}3^-$ mesoderm populations but decreases $CXCR4^+KDR^-$ endoderm populations.

Tracking germ layer differentiation through gene expression kinetics

Kinetic analyses can also be performed during the differentiation assays. By keeping BMP-4 constant at 10 ng/ml, four of the previously screened induction conditions were chosen in which two were optimal for endoderm (activin A at 20 ± 10 ng/ml VEGF) and two were optimal for mesoderm (activin A at 0 ± 10 ng/ml VEGF). All conditions were carried out on a single 96-well plate. Gene expression profiles were determined from cells obtained during the 6 days of differentiation. Genes expressed during mesoderm and endoderm induction were analyzed, with the inclusion of *OCT4* as a marker of pluripotency in undifferentiated cells.

Mesoderm genes (*KDR*, *PDGFRα*, *MEOX1*, *CD34*) were consistently expressed at higher levels in the absence of activin A while endoderm genes (*FOXA2*, *CXCR4*, *SOX17*) were consistently expressed in the presence of activin A (Fig. 5). *OCT4* expression steadily decreased under all conditions over the 6-day period. *Brachyury* expression peaked rapidly at Days 2–4 and then decreased in all samples, indicative of ESCs passing through the primitive streak stage (Fehling et al., 2003; Gadue et al., 2006; Wang and Nakayama, 2009). Additionally, non-activin A conditions demonstrated a clear progression through a $Brachyury^+KDR^-$ stage to a $Brachyury^+KDR^+$ stage, indicative of premesoderm to mesoderm/hemangioblast differentiation (Nostro et al., 2008; Fehling et al., 2003). *PDGFRα* is a marker of mesendoderm (Tada et al., 2005) and was expressed in all samples at Day 4 followed by increased expression in mesoderm inducing conditions. *CXCR4*, while expressed 100-fold higher in the activin A conditions, was still upregulated 10-fold in the absence of activin A when compared to undifferentiated cells. This is to be expected since *CXCR4* is not entirely endoderm specific but is also expressed by migrating mesoderm (McGrath et al., 1999). This result is consistent with CXCR4 protein expression detected by flow cytometry (Fig. S1A). Generally, the addition of VEGF had no notable effect on gene expression, with the exception of lateral (CD34) and paraxial (PDGFRα) specific genes. The expression of *CD34*, a lateral mesoderm and hematopoietic cell marker, was

Figure 2 Biomarker time course and germ layer gene expression analyses. Germ layer differentiation was initiated at Day 0. SSEA-3, NCAM, CXCR4, and KDR surface marker expression levels were assessed with flow cytometry at Days 0, 2, 4, and 6. (A) Endoderm differentiation flow cytometry profiles. Colored quadrants represent undifferentiated cells (brown) and differentiation to endoderm (blue), ectoderm (yellow), and mesoderm (red). Similar mesoderm and ectoderm plots are given in Fig. S1. (B) Marker expression profiles for all differentiation conditions over 6 days of differentiation. (C–F) RNA was prepared from cells harvested at Day 0 (hESCs) or Day 6 and analyzed for genes characteristic of pluripotency (C), endoderm (D), mesoderm (E), or ectoderm (F) by qPCR. Expression was normalized to the housekeeping gene *GAPDH* and all values are relative to hESC expression at Day 0. Error bars represent mean ± SD of three pooled wells from a single plate assay. Abbreviations: hESCs, human embryonic stem cells; BMP, bone morphogenetic protein; SSEA-3, stage-specific embryonic antigen-3; CXCR, CXC chemokine receptor; KDR, kinase insert domain receptor; NCAM, neural cell adhesion molecule; BMPR, bone morphogenetic protein receptor.

induced in the absence of activin A but only in the presence of VEGF. Conversely, the expression of the paraxial gene, *PDGFRα*, was highest in the absence of activin and VEGF, indicating that VEGF drives lateral or hematopoietic differentiation (Sakurai et al., 2006).

siRNA knockdown during endoderm differentiation

In addition to the amount of information that can be derived using this 96-well format in optimizing growth factor conditions and kinetics, this format is ideal as a high-throughput siRNA

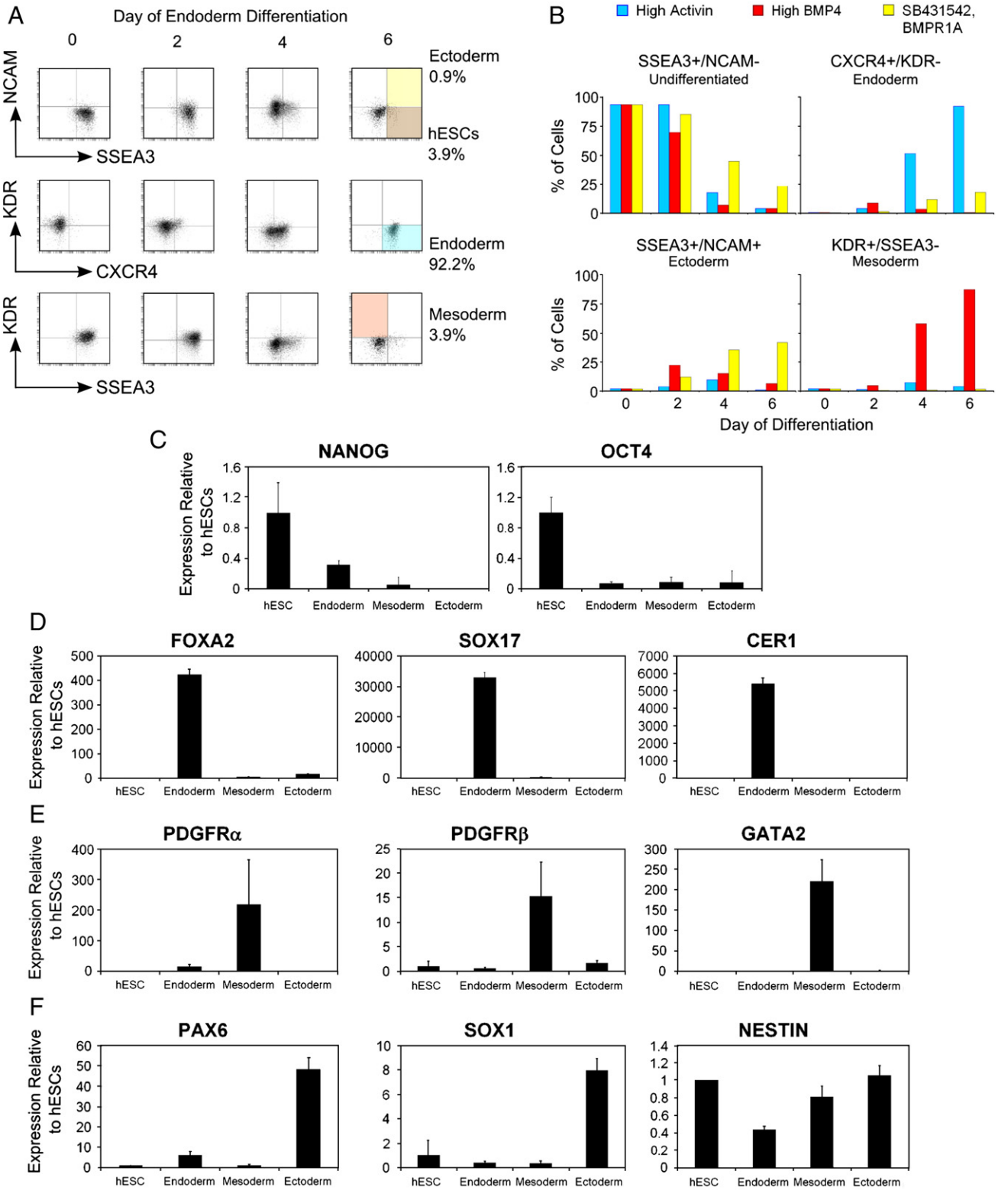

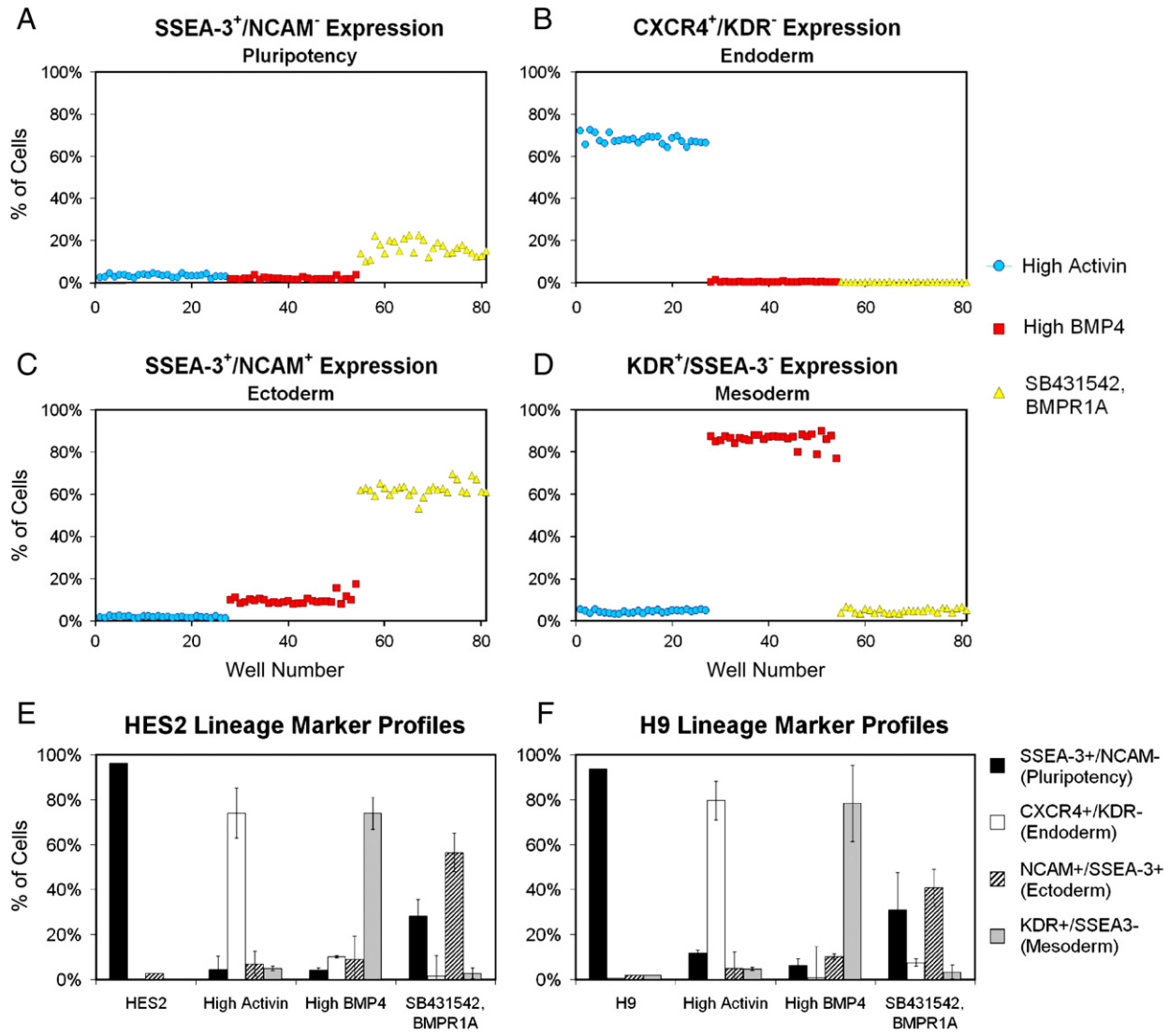

Figure 3 Day 6 phenotypes after differentiation to the three germ layers. (A–D) Interwell variability for 96-well flow cytometry expression profiles. hESCs were seeded into a 96-well plate and differentiated to endoderm, mesoderm, or ectoderm. Cells were stained for SSEA-3, CXCR4, NCAM, and KDR after 6 days to assess interwell variability and the ability to distinguish the separate germ layers. Plots show percentages of cells expressing the designated surface marker. (E–F) Biomarker profiles for HES2 and H9 differentiation. Each of the four cell types (hESCs, endoderm, mesoderm, ectoderm) was characterized by a unique biomarker expression profile. The 96-well format demonstrated highly efficient differentiation to all three lineages. Error bars represent well means of (E) two independent experiments ($n=2$) ± SD and (F) three independent experiments ($n=3$) ± SD. Each germ layer was significantly different for its appropriate biomarker at the $P<0.01$ level (Student's t test). Abbreviations: hESCs, human embryonic stem cells; SSEA-3, stage-specific embryonic antigen-3; CXCR, CXC chemokine receptor; KDR, kinase insert domain receptor; NCAM, neural cell adhesion molecule; BMPR, bone morphogenetic protein receptor.

screening platform during the differentiation of hESCs. To verify that siRNA knockdown can be achieved in this 96-well format without disrupting differentiation, hESCs that constitutively express an RFP protein (Irion et al., 2007) were utilized. These cells were induced to differentiate using endoderm conditions and transfected with a siRNA molecule targeting the *RFP* mRNA at day 1. Following 6 days of differentiation, cells were analyzed using flow cytometry and qPCR. Both control and mock-treated cells vividly fluoresced after 6 days, whereas cells exposed to the si*RFP* molecule only expressed very low levels of fluorescence (Fig. 6A). To evaluate RFP protein expression during endoderm induction, both RFP and CXCR4 expressions were analyzed using flow cytometry (Fig. 6B). Approximately 85% of both the control cells and the cells transfected with scrambled siRNA were RFP$^+$, compared to 4% of the cells transfected with siRNA targeted to RFP. Under all conditions, 75–80% of the cells were CXCR4$^+$, with no notable decrease caused by siRFP knockdown. To further verify that siRNA knockdown had not altered endoderm differentiation, qPCR analysis was performed after 6 days of differentiation (Fig. 6C) to analyze *RFP* expression and the anterior primitive streak/definitive endoderm markers *FOXA2* and *CER1*. *RFP*

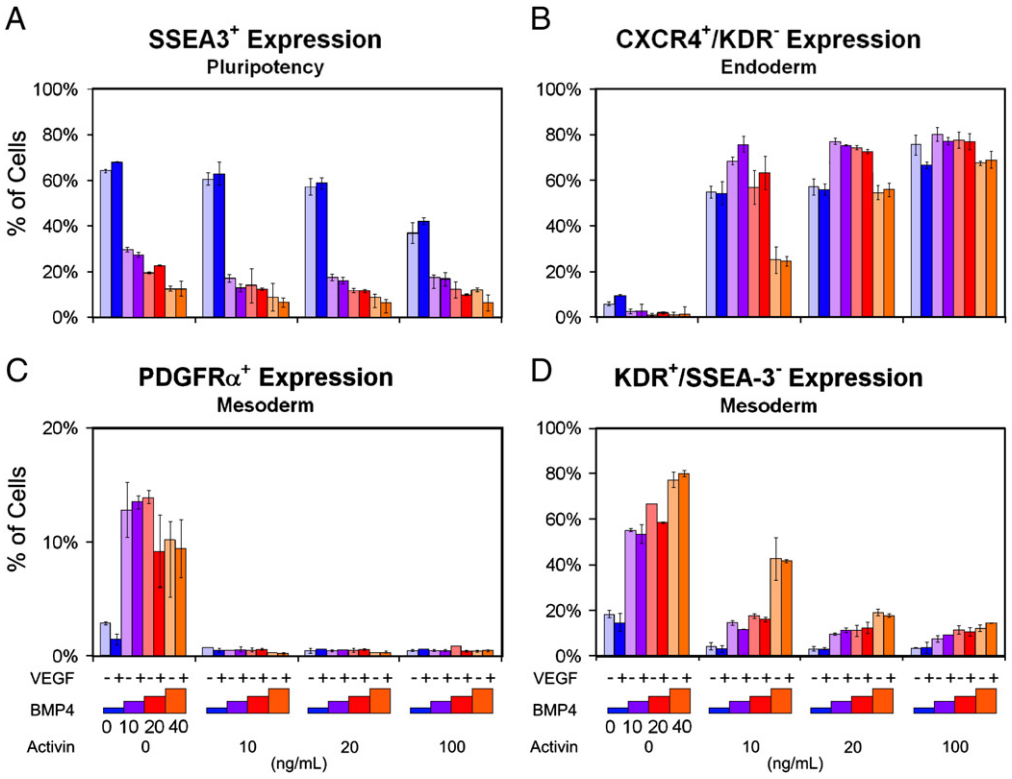

Figure 4 A 96-well plate growth factor screening analysis. Activin A, BMP4, and VEGF concentrations were varied over a 96-well plate and SSEA-3$^+$ (A), CXCR4$^+$KDR$^-$ (B), PDGFRα^+ (C), and KDR$^+$SSEA-3$^-$ (D) expression levels were analyzed using flow cytometry after 6 days of differentiation. All samples contained bFGF (Days 1–4, 2.5 ng/ml; Days 4–6, 5 ng/ml). VEGF concentration was ± 10 ng/ml. (A) Pluripotency decreased with increasing activin A and BMP4. (B) Endoderm populations increased with increasing activin A and decreased with increasing BMP4. (C, D) Mesoderm character was highest in the absence of activin A. PDGFRa$^+$ mesoderm was only detectable with no activin. KDR$^+$SSEA-3$^-$ mesoderm populations consistently increased with increasing BMP4 concentration and decreasing activin A concentration. All concentrations are ng/ml. Error bars represent the mean of two wells ± SD from a single plate assay. Abbreviations: SSEA-3, stage-specific embryonic antigen-3; CXCR, CXC chemokine receptor; KDR, kinase insert domain receptor; PDGFRα, platelet-derived growth factor-α; BMP, bone morphogenetic protein; VEGF, vascular endothelial growth factor.

transcript expression decreased by 96% as a result of siRNA knockdown. Neither *FOXA2* nor *CER1* expression were notably influenced by siRNA knockdown. These data suggest that siRNA knockdown can be performed in a 96-well format without significantly altering targeted differentiation.

Discussion

Serum-free and feeder-free hESCs differentiation protocols are essential in order to (1) maximize experimental control and reproducibility and (2) develop clinically applicable regenerative therapies (Chase and Firpo, 2007). Many studies have focused on titrating growth factors and inhibitors within SFD cocktails to optimize target cell differentiation. As lineages are further explored, the possible combinations of factors will inevitably rise. Screening assays are extremely effective in this pursuit. We have developed a high-throughput, multicolor flow cytometry assay of hESC differentiation that can be utilized to assess a range of SFD conditions. This small-scale format requires approximately 92% less reagents and growth factors than 6-well culture conditions and occupies 6% of the incubator space. Additionally, this assay utilizes surface markers to allow for live-cell analysis and sorting.

We differentiated hESCs to the three primary germ layers in this system, identified extracellular biomarker profiles for each, and confirmed germ layer identity with gene expression analysis. A wide variety of extra- and intracellular markers have been previously utilized to identify each of the primary germ layers. Given the heterogeneous expression patterns of endoderm, mesoderm, and ectoderm, no four-marker combination will perfectly distinguish all cells within each lineage. CXCR4 is expressed in migrating early endoderm and mesoderm (McGrath et al., 1999), developing vascular endothelial cells (Tachibana et al., 1998), and migrating neural stem cells (Imitola et al., 2004). Although typically 20–25% of mesodermal cells expressed CXCR4, our results showed that endoderm was uniquely distinguishable by CXCR4$^+$KDR$^-$ expression at this stage of differentiation. KDR is expressed on mesoderm cells after exiting the primitive streak (Ema et al., 2006) and has been utilized to characterize hESC differentiation to general mesoderm as well as vascular and cardiac progenitors (Nostro et al., 2008; Sakurai et al., 2006; Kattman et al., 2006). Although our results corresponded with previous

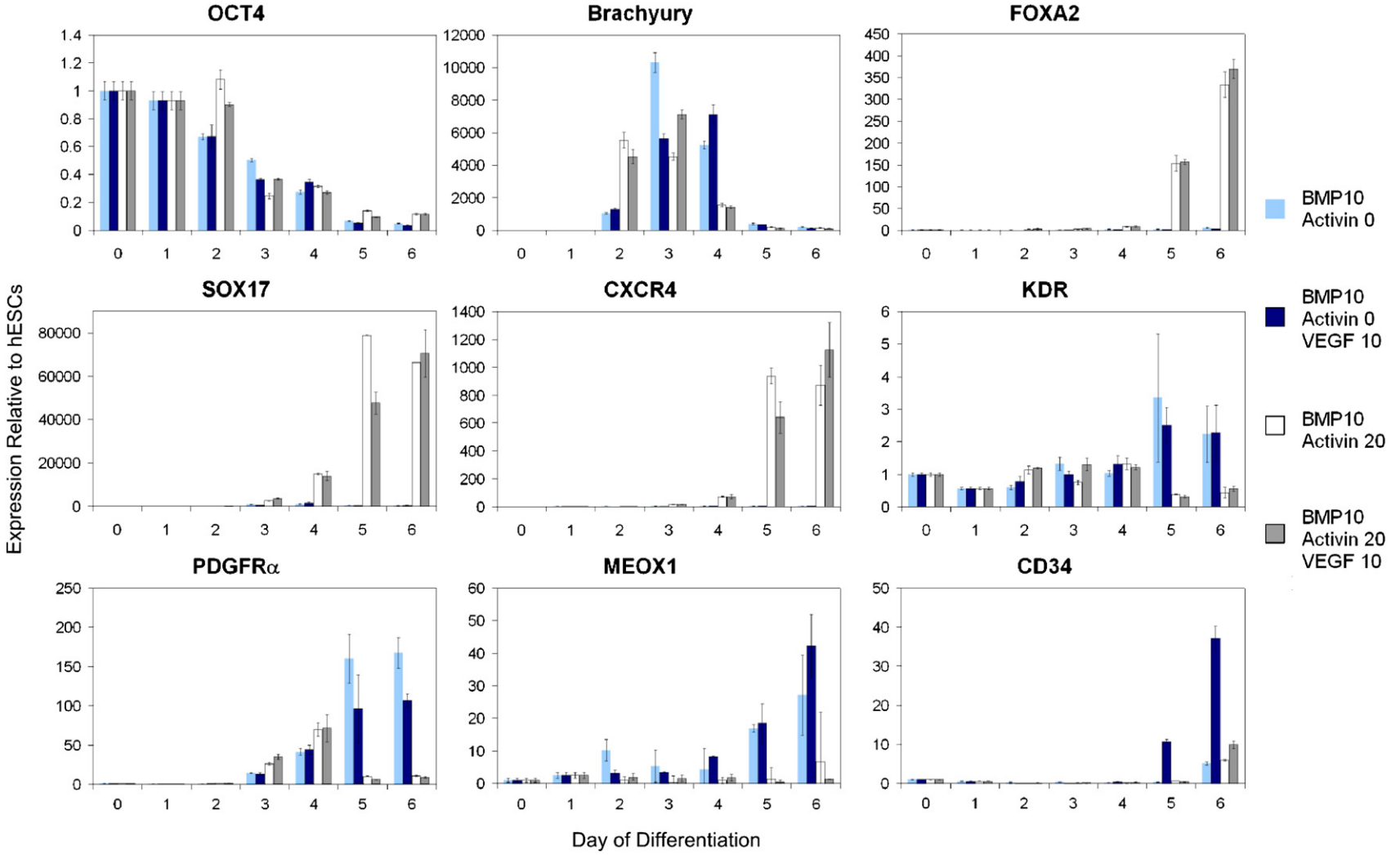

Figure 5 Gene expression kinetic analysis. Four conditions (10 ng/ml BMP4, ± 20 ng/ml activin A, ± 10 ng/ml VEGF) were chosen from the results of the growth factor screening experiment (Fig. 4) and analyzed for transcript expression levels during the 6-day differentiation procedure. Pluripotency (*OCT4*) decreased over differentiation and *Brachyury* expression peaked between 2 and 4 days. Endoderm genes (*FOXA2*, *CXCR4*, *SOX17*) were expressed much higher for conditions supplemented with activin A, whereas mesoderm gene expression (*KDR*, *PDGFRα*, *MEOX1*, *CD34*) was highest for non-activin A conditions. VEGF increased *CD34* and decreased *PDGFRα* expression at late time points. Expression was normalized to the housekeeping gene *GAPDH* and all values are relative to hESC expression at Day 0. Error bars represent mean ± SD of three pooled wells from a single plate assay. Abbreviations: hESCs, human embryonic stem cells; SSEA-3, stage-specific embryonic antigen-3; CXCR, CXC chemokine receptor; KDR, kinase insert domain receptor; NCAM, neural cell adhesion molecule; BMP, bone morphogenetic protein; VEGF, vascular endothelial growth factor.

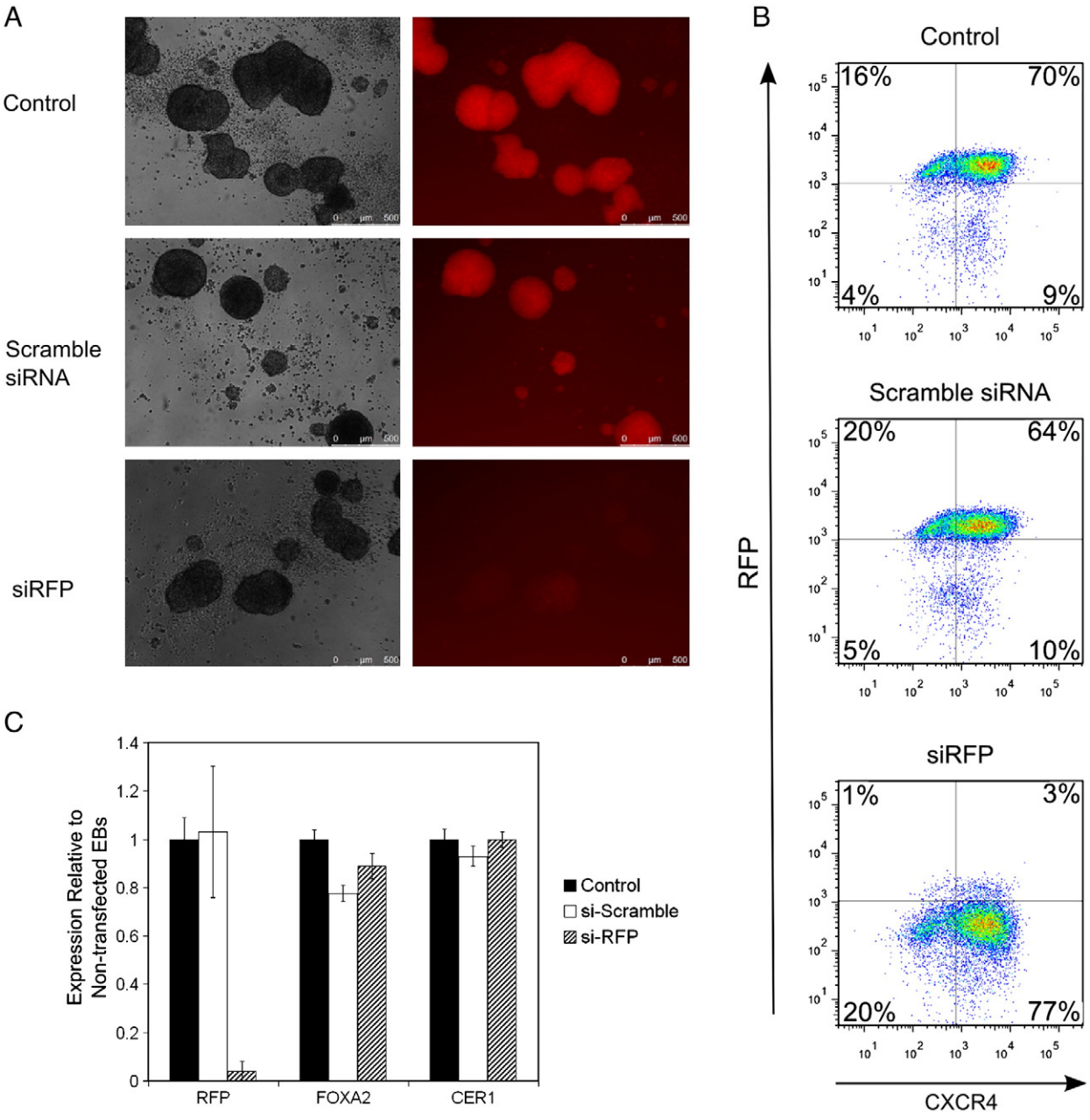

Figure 6 siRNA-mediated RFP knockdown during endoderm differentiation. hESCs were reverse-transfected with siRFP or a scrambled control when seeded into a 96-well plate format and induced to form endoderm in high activin A SFD media. (A) Fluorescence microscopy of Day 6 EBs. (B) Flow cytometry of Day 6 cells showing RFP (*y*-axis) vs CXCR4 (*x*-axis) expression. CXCR4 expression was not diminished by siRNA-induced RFP knockdown. (C) Gene expression analysis. qPCR was performed at Day 6 to analyze *RFP* transcript expression as well as the endoderm genes *FOXA2* and *CER1*. *RFP* knockdown had no notable effect on endoderm differentiation. Error bars represent mean ± SD of three pooled wells from a single plate assay. Abbreviations: EBs, embryoid bodies; RFP, red fluorescent protein; SFD, serum-free differentiation; CXCR, CXC chemokine receptor.

studies that have found KDR expression in a portion of hESCs (Yang et al., 2008), mesodermal cells generated by high BMP4 conditions were uniquely identifiable by $KDR^{+}SSEA\text{-}3^{-}$ expression. Currently, no well-characterized extracellular early ectoderm surface markers have been validated. Ectoderm has typically been characterized by the intracellular markers Nestin, β-III Tubulin, or Sox1 (Vallier et al., 2009; King et al., 2009; Nakagawa et al., 2008; Parekkadan et al., 2008; Smith et al., 2008; Watanabe et al., 2005). We exploited the delayed expression of SSEA-3 into the early neural stem cell stage (Pruszak et al., 2007) to overcome the confounding NCAM expression in endoderm and mesoderm. Transcript expression indicated that this stage is similar to the primitive anterior neuroectoderm/neuroepithelia stage defined by Pankratz et al. (Pankratz et al., 2007), namely that PAX6 expression is upregulated with SOX1 expression beginning to increase. This strategy carries the caveat that $SSEA\text{-}3^{+}NCAM^{+}$ phenotyping would not be applicable at a

later stage in the ectoderm lineage due to the loss of SSEA-3 expression.

Although exact comparisons are difficult to make due to various time points, markers utilized, data reported, and host species differences, we obtained excellent yields in relation to previous studies. Serum-containing, high activin A protocols have produced SOX17$^+$ endoderm yields ranging from 55% (Borowiak et al., 2009) to greater than 80% (D'Amour et al., 2005) after 5–6 days of differentiation in hESCs. Our yield of 80% for H9 cells falls within the higher range of this spectrum. Day 6 KDR$^+$ mesoderm populations of 15–25% (Goldman et al., 2009) and 52% (Zhang et al., 2008) cells have been obtained from hESCs. We obtained greater than 74% KDR$^+$SSEA-3$^-$ mesoderm yields for multiple hESC lines. Patani et al. generated Day 4 and Day 8 yields of 51% and approximately 80%, respectively, for cells positive for the neuroectoderm marker MUSASHI from hESCs (Patani et al., 2009). Chambers et al. generated greater than 80% HES5$^+$ neuroectoderm after 11 days of hESC differentiation (Chambers et al., 2009). Our 6-day protocol generated yields of 41–57%, comparable to these studies given the shorter time duration.

Many cytokine conditions, small molecules, and transfection conditions may induce cellular toxicity. Additionally, seeding densities may be highly variable due to the inability to seed hESCs as single cell suspensions in many lines. It is vital to obtain consistent and reliable results from a screening assay despite these caveats. This small-scale culture system demonstrated remarkable interwell repeatability and density robustness, particularly since static EB differentiation systems have been reported to generate highly heterogeneous cell populations (Carpenedo et al., 2007). Since 96- and 384-plate assays can display variations due to edges, evaporation, thermal variations, and pipetting error (Armknecht et al., 2005; Barker and Diamond, 2008; Faessel et al., 1999), we utilized gas-permeable membranes and stainless-steel lids to minimize evaporation and ensure a uniform heat distribution (Lucumi et al., 2010). All standard deviations were less than 4% for biomarker signals, which allowed for highly significant differences between conditions.

While many studies have utilized siRNA as a tool for studying ESC differentiation, there are limited data reporting the presence or absence of off-target siRNA effects on differentiation outcome. Nonviral transfection of off-target siRNA molecules has been found to induce adipogenesis in human mesenchymal stem cells (Xu et al., 2007). Hence, it is important to measure the effects that transfection or transduction may induce in ESC differentiation protocols. We found that siRNA-mediated knockdown of constitutively expressed RFP was highly efficient and induced no notable effects on endoderm differentiation. Cells were transfected with the siRNA molecules at Day 1 of differentiation and exhibited significant RFP knockdown at Day 6. This assay provides a siRNA screening platform that can potentially be utilized for differentiation pathway analysis.

In an effort to demonstrate the efficiency and power of this 96-well assay system, we conducted a growth factor screening assay utilizing a single 96-well plate and analyzed 32 conditions in duplicate. We then extended the capabilities of this small-scale system to analyze time-course gene expression profiles for four of these conditions, again, within a single 96-well plate. bFGF in combination with activin A or BMP4 drove differentiation and reduced pluripotency. In particular, the greatest number of CXCR4$^+$KDR$^-$ cells was induced by low to high activin A with no BMP4. Gene profiles over the 6-day time period for the activin A + BMP4 conditions confirmed that these CXCR4$^+$KDR$^-$ cells were characteristic of definitive endoderm. These results correspond to previous studies that found increased CXCR4 expression and increased definitive endoderm yields by differentiating cells under high activin A containing SFD conditions (D'Amour et al., 2005; Yao et al., 2006). Our results are similar to those of Vallier et al. in which high activin A in combination with bFGF and BMP4 induced mesendoderm (Vallier et al., 2009). Several studies have previously reported that activin A + bFGF blocks differentiation and maintains pluripotency (Vallier et al., 2009; Xiao et al., 2006), whereas our results demonstrated increased endoderm production. Our protocol includes a BMP4 exposure step at Day 0–1 to serve as a "jumpstart" to differentiation. The decrease in pluripotent marker expression in subsequent activin A + bFGF SFD conditions is likely attributable to this step. Activin A and BMP4 exhibited a competitive effect on mesoderm marker expression. The presence of activin A alone eliminated PDGFRα expression at Day 6, although all samples demonstrated transcript expression through the Day 2–4 primitive streak stage. This PDGFRα reducing effect of activin A has been previously observed (Vallier et al., 2009). Similarly, activin A reduced KDR$^+$SSEA-3$^-$ expression, with highest expression levels seen under high BMP4 SFD conditions with no activin A. These results also corroborate previous studies that have induced mesoderm and vascular progenitors through BMP4 activation (Park et al., 2004; Bai et al., 2010) and noted reduced KDR expression with increasing activin A supplementation (Yang et al., 2008; Nostro et al., 2008; Vallier et al., 2009).

The addition of VEGF to SFD had no notable effect on surface marker expression at Day 6. However, *CD34* transcript expression increased and *PDGFRα* expression decreased, indicating a role in inducing early mesoderm cells toward a hematopoietic lineage. Indeed, several studies have utilized VEGF to induce mesendoderm or mesoderm progenitors toward a hematopoietic or cardiovascular state (Pick et al., 2007; Yang et al., 2008; Narazaki et al., 2008), and VEGF inclusion has been shown to improve subsequent hematopoietic blast colony formation (Nostro et al., 2008).

Elucidating the optimal serum-free protocols for EB differentiation of hESCs will require exploring a vast combinatorial field of growth factors, inhibitors, and cytokines. This small-scale culture platform and live-cell flow assay provides a more efficient and more cost-effective approach to analyzing a large number of conditions. It can additionally be utilized to discover biological pathways or optimize differentiation through RNAi or miRNA screens. By varying biomarkers, this assay can be adopted to various stages of lineage differentiation to significantly enhance progress toward hESC-derived clinical therapies.

Materials and methods

hESC maintenance

HES2 (passage 26–34) and H9 cells (passage 35–45) were maintained on irradiated mouse embryonic fibroblasts (MEFs) in DMEM/F12 50/50 (Mediatech) supplemented with 20% Knockout

Serum (Invitrogen, Carlsbad, CA), 1X nonessential amino acids (Invitrogen), 0.55 mM β-mercaptoethanol, 1% penicillin/streptomycin, 2 mM glutamine (Invitrogen), and 20 ng/ml bFGF (R&D Systems, Minneapolis, MN). Cells were passaged at 1:3–1:6 ratios using 0.25% trypsin/EDTA (Mediatech, Manassas, VA). For siRNA experiments, a previously established HES2 line was utilized that expresses a red fluorescent protein (RFP) from the *hROSA26* locus (HES2-R26) (Irion et al., 2007).

hESC differentiation

A 6-day differentiation procedure was utilized (Fig. 1A). Prior to differentiation, hESCs were trypsinized and replated on matrigel (Becton Dickinson, Franklin Lakes, NJ). SFD medium consisted of 75% IMDM (Invitrogen), 25% F12 (Mediatech), 0.5X N-2 supplement (Invitrogen), 0.5X B27 without retinoic acid (Invitrogen), and 0.05% BSA (Sigma, St. Louis, MO). On 75% confluency, cells were trypsinized, harvested with a cell scraper, spun down, and resuspended in SFD medium supplemented with penicillin/streptomycin, 2 mM glutamine, 0.5 mM ascorbic acid (Sigma), 1.5×10^{-4} M monothioglycerol (Sigma), and the specified concentrations of cytokines as indicated (summarized in Table 1). Day 0 media were supplemented with 10 ng/ml BMP4 (R&D Systems) for endoderm/mesoderm or 10 μM SB431542 (Tocris, Ellisville, MO), 500 ng/ml BMPR1A (R&D Systems), and 5 ng/ml bFGF (R&D Systems, Minneapolis, MN) for ectoderm. Cells (2×10^6) were seeded into 10-cm petri dishes and cultured at 5% CO_2/5% O_2/90% N_2. After 24 h, EBs were harvested, manually disrupted, and seeded into 100 μl Day 1 medium into low-cluster 96-well plates (Corning, Corning, NY) at 2×10^5 cells/ml (2×10^4 cells/well). Endoderm Day 1 medium was supplemented with 100 ng/ml activin A (R&D Systems), 2.5 ng/ml bFGF, 0.5 ng/ml BMP4. Mesoderm Day 1 medium was supplemented with 0.5 ng/ml activin A, 2.5 ng/ml bFGF, and 20 ng/ml BMP4. Ectoderm Day 1 medium was supplemented with 5 ng/ml bFGF, 10 μM SB431542, and 500 ng/ml BMPR1A. For growth factor screening experiments, Day 1 media contained 2.5 ng/ml bFGF, and activin A and BMP4 were utilized at concentrations of 0 to 100 ng/ml, as indicated. At Day 4, 200 μl of Day 4 media was added to each well. Day 4 mesoderm and endoderm media were identical to Day 1 media, but with 5 ng/ml bFGF. Day 4 ectoderm medium was identical to Day 1 medium with 20 ng/ml bFGF. For growth factor screening experiments, media were supplemented with 5 ng/ml bFGF, the indicated concentrations of activin A and BMP4, and ± 10 ng/ml VEGF (R&D Systems). During incubation, 96-well plates were covered with gas-permeable membranes (Breathe Easy, Diversified Biotech, Boston, MA) and stainless-steel plate lids (Kalypsys, Inc., San Diego, CA).

Ninety-six well flow cytometry

EBs were dissociated with 0.25% trypsin/EDTA. Antibodies utilized were as follows: rat anti-SSEA-3-Alexa 488 (Biolegend, San Diego, CA, 330306), mouse anti-CXCR4-PE (Invitrogen, MHCCXCR404), mouse anti-NCAM-PE/Cy7 (Biolegend, 318318), mouse anti-KDR-Alexa 647 (Biolegend, 338909), mouse anti-PDGFRα-biotin (Biolegend, 323503), and streptavidin-PE/Cy7 (Invitrogen, SA1012). Cells were acquired directly from 96-well plates using a C6 flow cytometer equipped with a 96-well plate C-Sampler (Accuri, Ann Arbor, MI) and analyzed using CFlow Plus software (Accuri) or FlowJo (Treestar, Ashland, OR).

Real-time quantitative PCR

EBs were collected from wells and dissociated with 0.25% trypsin/EDTA. Cells were lysed with the facilitation of

Table 1 Differentiation media

	Day 0	Day 1	Day 4
Endoderm	•2 mM glutamine (Invitrogen) •0.5 mM ascorbic acid (Sigma) •1.5×10^{-4} M monothioglycerol (Sigma) •10 ng/ml BMP4 (R&D Systems)	•2 mM glutamine •0.5 mM ascorbic acid •1.5×10^{-4} M monothioglycerol •0.5 ng/ml BMP4 •100 ng/ml activin A (R&D Systems) •2.5 ng/ml bFGF (R&D Systems)	•2 mM glutamine •0.5 mM ascorbic acid •1.5×10^{-4} M monothioglycerol •0.5 ng/ml BMP4 •100 ng/ml activin A •5 ng/ml bFGF
Mesoderm	Identical to Day 0 endoderm	•2 mM glutamine •0.5 mM ascorbic acid •1.5×10^{-4} M monothioglycerol •20 ng/ml BMP4 •0.5 ng/ml activin A •2.5 ng/ml bFGF	•2 mM glutamine •0.5 mM ascorbic acid •1.5×10^{-4} M monothioglycerol •20 ng/ml BMP4 •0.5 ng/ml activin A •5 ng/ml bFGF
Ectoderm	•2 mM glutamine •0.5 mM ascorbic acid •1.5×10^{-4} M monothioglycerol •500 ng/ml BMPR1A (R&D Systems) •10 μM SB431542 (Tocris) •5 ng/ml bFGF	Identical to Day 0 ectoderm	•2 mM glutamine •0.5 mM ascorbic acid •1.5×10^{-4} M monothioglycerol •500 ng/ml BMPR1A •10 μM SB431542 •20 ng/ml bFGF

QiaShredder columns and RNA was harvested using an RNeasy Mini-kit and treated with RNase-free DNase (Qiagen, Valencia, CA). Reverse transcription was performed with the iScript cDNA synthesis kit (Bio-Rad, Hercules, CA) or the High Capacity cDNA Reverse Transcription kit (Applied Biosystems). Real-time quantitative PCR (qPCR) was performed in triplicate on a Roche Lightcycler 480 using LightCycler 480 SYBR Green I master mix (Roche, Indianapolis, IN) and 500 nM primer concentrations (Table S1). All gene expression levels were normalized to the housekeeping gene *GAPDH* (Pick et al., 2007).

siRNA knockdown

HES2 cells stably expressing RFP (HES2-R26 cells) (Irion et al., 2007) were reverse-transfected at the time of 96-well plate seeding at Day 1. Cells (2×10^4) in 100 μl of Day 1 endoderm media were seeded onto a 20 μl transfection volume of Optimem I Reduced Serum Media (Invitrogen) containing 0.2 μl RNAiMax per well (Invitrogen) and 10 nM of either a nonspecific scramble siRNA (Applied Biosystems, Foster City, CA) or a siRNA designed to target the *RFP* mRNA (IDT, Coralville, IA). Day 1 total well volume was thus 120 μl. Control samples were seeded into Optimem Media. RNAiMax was utilized due to its high efficiency of delivering siRNA into hESCs (Zhao et al., 2008). Differentiation was performed as previously described, in which 200 μl medium at Day 4 was subsequently added to each well.

Supplementary data associated with this article can be found, in the online version, at doi:10.1016/j.scr.2010.11.001.

Acknowledgments

The authors thank the Children's Hospital of Philadelphia hESC/iPS Core facility for its generous use of facilities and resources and invaluable guidance.

References

Armknecht, S., Boutros, M., Kiger, A., Nybakken, K., Mathey-Prevot, B., Perrimon, N., 2005. High-throughput RNA interference screens in Drosophila tissue culture cells. Meth. Enzymol. 392, 55–73.

Bai, H., Gao, Y., Arzigian, M., Wojchowski, D.M., Wu, W.S., Wang, Z.Z., 2010. BMP4 regulates vascular progenitor development in human embryonic stem cells through a smad-dependent pathway. J. Cell. Biochem. 109, 363–374.

Barker, G.A., Diamond, S.L., 2008. RNA interference screen to identify pathways that enhance or reduce nonviral gene transfer during lipofection. Mol. Ther. 16, 1602–1608.

Borowiak, M., Maehr, R., Chen, S., Chen, A.E., Tang, W., Fox, J.L., Schreiber, S.L., Melton, D.A., 2009. Small molecules efficiently direct endodermal differentiation of mouse and human embryonic stem cells. Cell Stem Cell 4, 348–358.

Carpenedo, R.L., Sargent, C.Y., McDevitt, T.C., 2007. Rotary suspension culture enhances the efficiency, yield, and homogeneity of embryoid body differentiation. Stem Cells 25, 2224–2234.

Chambers, S.M., Fasano, C.A., Papapetrou, E.P., Tomishima, M., Sadelain, M., Studer, L., 2009. Highly efficient neural conversion of human ES and iPS cells by dual inhibition of SMAD signaling. Nat. Biotechnol. 27, 275–280.

Chase, L.G., Firpo, M.T., 2007. Development of serum-free culture systems for human embryonic stem cells. Curr. Opin. Chem. Biol. 11, 367–372.

D'Amour, K.A., Agulnick, A.D., Eliazer, S., Kelly, O.G., Kroon, E., Baetge, E.E., 2005. Efficient differentiation of human embryonic stem cells to definitive endoderm. Nat. Biotechnol. 23, 1534–1541.

D'Amour, K.A., Bang, A.G., Eliazer, S., Kelly, O.G., Agulnick, A.D., Smart, N.G., Moorman, M.A., Kroon, E., Carpenter, M.K., Baetge, E.E., 2006. Production of pancreatic hormone-expressing endocrine cells from human embryonic stem cells. Nat. Biotechnol. 24, 1392–1401.

Davis, R.P., Ng, E.S., Costa, M., Mossman, A.K., Sourris, K., Elefanty, A.G., Stanley, E.G., 2008. Targeting a GFP reporter gene to the MIXL1 locus of human embryonic stem cells identifies human primitive streak-like cells and enables isolation of primitive hematopoietic precursors. Blood 111, 1876–1884.

Desbordes, S.C., Placantonakis, D.G., Ciro, A., Socci, N.D., Lee, G., Djaballah, H., Studer, L., 2008. High-throughput screening assay for the identification of compounds regulating self-renewal and differentiation in human embryonic stem cells. Cell Stem Cell 2, 602–612.

Ema, M., Takahashi, S., Rossant, J., 2006. Deletion of the selection cassette, but not cis-acting elements, in targeted Flk1-lacZ allele reveals Flk1 expression in multipotent mesodermal progenitors. Blood 107, 111–117.

Enver, T., Soneji, S., Joshi, C., Brown, J., Iborra, F., Orntoft, T., Thykjaer, T., Maltby, E., Smith, K., Dawud, R.A., Jones, M., Matin, M., Gokhale, P., Draper, J., Andrews, P.W., 2005. Cellular differentiation hierarchies in normal and culture-adapted human embryonic stem cells. Hum. Mol. Genet. 14, 3129–3140.

Faessel, H.M., Levasseur, L.M., Slocum, H.K., Greco, W.R., 1999. Parabolic growth patterns in 96-well plate cell growth experiments. In Vitro Cell. Dev. Biol. Anim. 35, 270–278.

Fehling, H.J., Lacaud, G., Kubo, A., Kennedy, M., Robertson, S., Keller, G., Kouskoff, V., 2003. Tracking mesoderm induction and its specification to the hemangioblast during embryonic stem cell differentiation. Development 130, 4217–4227.

Gadue, P., Huber, T.L., Nostro, M.C., Kattman, S., Keller, G.M., 2005. Germ layer induction from embryonic stem cells. Exp. Hematol. 33, 955–964.

Gadue, P., Huber, T.L., Paddison, P.J., Keller, G.M., 2006. Wnt and TGF-beta signaling are required for the induction of an in vitro model of primitive streak formation using embryonic stem cells. Proc. Natl. Acad. Sci. USA 103, 16806–16811.

Goldman, O., Feraud, O., Boyer-Di Ponio, J., Driancourt, C., Clay, D., Le Bousse-Kerdiles, M.C., Bennaceur-Griscelli, A., Uzan, G., 2009. A boost of BMP4 accelerates the commitment of human embryonic stem cells to the endothelial lineage. Stem Cells 27, 1750–1759.

Hay, D.C., Sutherland, L., Clark, J., Burdon, T., 2004. Oct-4 knockdown induces similar patterns of endoderm and trophoblast differentiation markers in human and mouse embryonic stem cells. Stem Cells 22, 225–235.

Imitola, J., Raddassi, K., Park, K.I., Mueller, F.J., Nieto, M., Teng, Y.D., Frenkel, D., Li, J., Sidman, R.L., Walsh, C.A., Snyder, E.Y., Khoury, S.J., 2004. Directed migration of neural stem cells to sites of CNS injury by the stromal cell-derived factor 1alpha/CXC chemokine receptor 4 pathway. Proc. Natl. Acad. Sci. USA 101, 18117–18122.

Irion, S., Luche, H., Gadue, P., Fehling, H.J., Kennedy, M., Keller, G., 2007. Identification and targeting of the ROSA26 locus in human embryonic stem cells. Nat. Biotechnol. 25, 1477–1482.

Izumi, N., Era, T., Akimaru, H., Yasunaga, M., Nishikawa, S., 2007. Dissecting the molecular hierarchy for mesendoderm differentiation through a combination of embryonic stem cell culture and RNA interference. Stem Cells 25, 1664–1674.

Kannagi, R., Cochran, N.A., Ishigami, F., Hakomori, S., Andrews, P.W., Knowles, B.B., Solter, D., 1983. Stage-specific embryonic antigens

(SSEA-3 and -4) are epitopes of a unique globo-series ganglioside isolated from human teratocarcinoma cells. EMBO J. 2, 2355–2361.

Kattman, S.J., Huber, T.L., Keller, G.M., 2006. Multipotent flk-1+ cardiovascular progenitor cells give rise to the cardiomyocyte, endothelial, and vascular smooth muscle lineages. Dev. Cell 11, 723–732.

Kennedy, M., D'Souza, S.L., Lynch-Kattman, M., Schwantz, S., Keller, G., 2007. Development of the hemangioblast defines the onset of hematopoiesis in human ES cell differentiation cultures. Blood 109, 2679–2687.

King, F.W., Ritner, C., Liszewski, W., Kwan, H.C., Pedersen, A., Leavitt, A.D., Bernstein, H.S., 2009. Subpopulations of human embryonic stem cells with distinct tissue-specific fates can be selected from pluripotent cultures. Stem Cells Dev. 18, 1441–1450.

Koike, M., Kurosawa, H., Amano, Y., 2005. A round-bottom 96-well polystyrene plate coated with 2-methacryloyloxyethyl phosphorylcholine as an effective tool for embryoid body formation. Cytotechnology 47, 3–10.

Koike, M., Sakaki, S., Amano, Y., Kurosawa, H., 2007. Characterization of embryoid bodies of mouse embryonic stem cells formed under various culture conditions and estimation of differentiation status of such bodies. J. Biosci. Bioeng. 104, 294–299.

Kyba, M., Perlingeiro, R.C., Daley, G.Q., 2002. HoxB4 confers definitive lymphoid-myeloid engraftment potential on embryonic stem cell and yolk sac hematopoietic progenitors. Cell 109, 29–37.

Lackie, P.M., Zuber, C., Roth, J., 1994. Polysialic acid of the neural cell adhesion molecule (N-CAM) is widely expressed during organogenesis in mesodermal and endodermal derivatives. Differentiation 57, 119–131.

Lendahl, U., Zimmerman, L.B., McKay, R.D., 1990. CNS stem cells express a new class of intermediate filament protein. Cell 60, 585–595.

Lucumi, E., Darling, C., Jo, H., Napper, A.D., Chandramohanadas, R., Fisher, N., Shone, A.E., Jing, H., Ward, S.A., Biagini, G.A., DeGrado, W.F., Diamond, S.L., Greenbaum, D.C., 2010. Discovery of potent small-molecule inhibitors of multidrug-resistant *Plasmodium falciparum* using a novel miniaturized high-throughput luciferase-based assay. Antimicrob. Agents Chemother. 54, 3597–3604.

Matsumoto, K., Isagawa, T., Nishimura, T., Ogaeri, T., Eto, K., Miyazaki, S., Miyazaki, J., Aburatani, H., Nakauchi, H., Ema, H., 2009. Stepwise development of hematopoietic stem cells from embryonic stem cells. PLoS ONE 4, e4820.

McGrath, K.E., Koniski, A.D., Maltby, K.M., McGann, J.K., Palis, J., 1999. Embryonic expression and function of the chemokine SDF-1 and its receptor, CXCR4. Dev. Biol. 213, 442–456.

Moller, C.J., Christgau, S., Williamson, M.R., Madsen, O.D., Niu, Z.P., Bock, E., Baekkeskov, S., 1992. Differential expression of neural cell adhesion molecule and cadherins in pancreatic islets, glucagonomas, and insulinomas. Mol. Endocrinol. 6, 1332–1342.

Nakagawa, M., Koyanagi, M., Tanabe, K., Takahashi, K., Ichisaka, T., Aoi, T., Okita, K., Mochiduki, Y., Takizawa, N., Yamanaka, S., 2008. Generation of induced pluripotent stem cells without Myc from mouse and human fibroblasts. Nat. Biotechnol. 26, 101–106.

Nakanishi, M., Kurisaki, A., Hayashi, Y., Warashina, M., Ishiura, S., Kusuda-Furue, M., Asashima, M., 2009. Directed induction of anterior and posterior primitive streak by Wnt from embryonic stem cells cultured in a chemically defined serum-free medium. FASEB J. 23, 114–122.

Narazaki, G., Uosaki, H., Teranishi, M., Okita, K., Kim, B., Matsuoka, S., Yamanaka, S., Yamashita, J.K., 2008. Directed and systematic differentiation of cardiovascular cells from mouse induced pluripotent stem cells. Circulation 118, 498–506.

Ng, E.S., Davis, R.P., Azzola, L., Stanley, E.G., Elefanty, A.G., 2005. Forced aggregation of defined numbers of human embryonic stem cells into embryoid bodies fosters robust, reproducible hematopoietic differentiation. Blood 106, 1601–1603.

Ng, E.S., Davis, R., Stanley, E.G., Elefanty, A.G., 2008. A protocol describing the use of a recombinant protein-based, animal product-free medium (APEL) for human embryonic stem cell differentiation as spin embryoid bodies. Nat. Protoc. 3, 768–776.

Nostro, M.C., Cheng, X., Keller, G.M., Gadue, P., 2008. Wnt, activin, and BMP signaling regulate distinct stages in the developmental pathway from embryonic stem cells to blood. Cell Stem Cell 2, 60–71.

Pankratz, M.T., Li, X.J., Lavaute, T.M., Lyons, E.A., Chen, X., Zhang, S.C., 2007. Directed neural differentiation of human embryonic stem cells via an obligated primitive anterior stage. Stem Cells 25, 1511–1520.

Parekkadan, B., Berdichevsky, Y., Irimia, D., Leeder, A., Yarmush, G., Toner, M., Levine, J.B., Yarmush, M.L., 2008. Cell-cell interaction modulates neuroectodermal specification of embryonic stem cells. Neurosci. Lett. 438, 190–195.

Park, C., Afrikanova, I., Chung, Y.S., Zhang, W.J., Arentson, E., Fong Gh, G., Rosendahl, A., Choi, K., 2004. A hierarchical order of factors in the generation of FLK1- and SCL-expressing hematopoietic and endothelial progenitors from embryonic stem cells. Development 131, 2749–2762.

Park, I.H., Zhao, R., West, J.A., Yabuuchi, A., Huo, H., Ince, T.A., Lerou, P.H., Lensch, M.W., Daley, G.Q., 2008. Reprogramming of human somatic cells to pluripotency with defined factors [see comment]. Nature 451, 141–146.

Patani, R., Compston, A., Puddifoot, C.A., Wyllie, D.J., Hardingham, G.E., Allen, N.D., Chandran, S., 2009. Activin/nodal inhibition alone accelerates highly efficient neural conversion from human embryonic stem cells and imposes a caudal positional identity. PLoS ONE [Electron. Resour.] 4, e7327.

Pick, M., Azzola, L., Mossman, A., Stanley, E.G., Elefanty, A.G., 2007. Differentiation of human embryonic stem cells in serum-free medium reveals distinct roles for bone morphogenetic protein 4, vascular endothelial growth factor, stem cell factor, and fibroblast growth factor 2 in hematopoiesis. Stem Cells 25, 2206–2214.

Pruszak, J., Sonntag, K.C., Aung, M.H., Sanchez-Pernaute, R., Isacson, O., 2007. Markers and methods for cell sorting of human embryonic stem cell-derived neural cell populations. Stem Cells 25, 2257–2268.

Reubinoff, B.E., Pera, M.F., Fong, C.Y., Trounson, A., Bongso, A., 2000. Embryonic stem cell lines from human blastocysts: somatic differentiation in vitro. Nat. Biotechnol. 18, 399–404.

Rodriguez, R.T., Velkey, J.M., Lutzko, C., Seerke, R., Kohn, D.B., O'Shea, K.S., Firpo, M.T., 2007. Manipulation of OCT4 levels in human embryonic stem cells results in induction of differential cell types. Exp. Biol. Med. 232, 1368–1380.

Sakurai, H., Era, T., Jakt, L.M., Okada, M., Nakai, S., Nishikawa, S., Nishikawa, S., 2006. In vitro modeling of paraxial and lateral mesoderm differentiation reveals early reversibility. Stem Cells 24, 575–586.

Smith, J.R., Vallier, L., Lupo, G., Alexander, M., Harris, W.A., Pedersen, R.A., 2008. Inhibition of activin/nodal signaling promotes specification of human embryonic stem cells into neuroectoderm. Dev. Biol. 313, 107–117.

Tachibana, K., Hirota, S., Iizasa, H., Yoshida, H., Kawabata, K., Kataoka, Y., Kitamura, Y., Matsushima, K., Yoshida, N., Nishikawa, S., Kishimoto, T., Nagasawa, T., 1998. The chemokine receptor CXCR4 is essential for vascularization of the gastrointestinal tract. Nature 393, 591–594.

Tada, S., Era, T., Furusawa, C., Sakurai, H., Nishikawa, S., Kinoshita, M., Nakao, K., Chiba, T., Nishikawa, S., 2005. Characterization of mesendoderm: a diverging point of the definitive endoderm and mesoderm in embryonic stem cell differentiation culture. Development 132, 4363–4374.

Vallier, L., Rugg-Gunn, P.J., Bouhon, I.A., Andersson, F.K., Sadler, A.J., Pedersen, R.A., 2004. Enhancing and diminishing gene function in human embryonic stem cells. Stem Cells 22, 2–11.

Vallier, L., Touboul, T., Chng, Z., Brimpari, M., Hannan, N., Millan, E., Smithers, L.E., Trotter, M., Rugg-Gunn, P., Weber, A., Pedersen, R.A., 2009. Early cell fate decisions of human embryonic stem cells and mouse epiblast stem cells are controlled by the same signalling pathways. PLoS ONE 4, e6082.

Wang, Y., Nakayama, N., 2009. WNT and BMP signaling are both required for hematopoietic cell development from human ES cells. Stem Cell Res. 3, 113–125.

Watanabe, K., Kamiya, D., Nishiyama, A., Katayama, T., Nozaki, S., Kawasaki, H., Watanabe, Y., Mizuseki, K., Sasai, Y., 2005. Directed differentiation of telencephalic precursors from embryonic stem cells. Nat. Neurosci. 8, 288–296.

Xiao, L., Yuan, X., Sharkis, S.J., 2006. Activin A maintains self-renewal and regulates fibroblast growth factor, Wnt, and bone morphogenic protein pathways in human embryonic stem cells. Stem Cells 24, 1476–1486.

Xu, Y., Mirmalek-Sani, S.H., Lin, F., Zhang, J., Oreffo, R.O., 2007. Adipocyte differentiation induced using nonspecific siRNA controls in cultured human mesenchymal stem cells. RNA 13, 1179–1183.

Yang, L., Soonpaa, M.H., Adler, E.D., Roepke, T.K., Kattman, S.J., Kennedy, M., Henckaerts, E., Bonham, K., Abbott, G.W., Linden, R.M., Field, L.J., Keller, G.M., 2008. Human cardiovascular progenitor cells develop from a KDR+ embryonic-stem-cell-derived population. Nature 453, 524–528.

Yao, S., Chen, S., Clark, J., Hao, E., Beattie, G.M., Hayek, A., Ding, S., 2006. Long-term self-renewal and directed differentiation of human embryonic stem cells in chemically defined conditions. Proc. Natl. Acad. Sci. USA 103, 6907–6912.

Yasunaga, M., Tada, S., Torikai-Nishikawa, S., Nakano, Y., Okada, M., Jakt, L.M., Nishikawa, S., Chiba, T., Era, T., Nishikawa, S., 2005. Induction and monitoring of definitive and visceral endoderm differentiation of mouse ES cells. Nat. Biotechnol. 23, 1542–1550.

Zaehres, H., Lensch, M.W., Daheron, L., Stewart, S.A., Itskovitz-Eldor, J., Daley, G.Q., 2005. High-efficiency RNA interference in human embryonic stem cells. Stem Cells 23, 299–305.

Zambidis, E.T., Peault, B., Park, T.S., Bunz, F., Civin, C.I., 2005. Hematopoietic differentiation of human embryonic stem cells progresses through sequential hematoendothelial, primitive, and definitive stages resembling human yolk sac development. Blood 106, 860–870.

Zhang, P., Li, J., Tan, Z., Wang, C., Liu, T., Chen, L., Yong, J., Jiang, W., Sun, X., Du, L., Ding, M., Deng, H., 2008. Short-term BMP-4 treatment initiates mesoderm induction in human embryonic stem cells. Blood 111, 1933–1941.

Zhao, M., Yang, H., Jiang, X., Zhou, W., Zhu, B., Zeng, Y., Yao, K., Ren, C., 2008. Lipofectamine RNAiMAX: an efficient siRNA transfection reagent in human embryonic stem cells. Mol. Biotechnol. 40, 19–26.